land

MDPI

Article

Diurnal Variation in Urban Heat Island Intensity in Birmingham: The Relationship between Nocturnal Surface and Canopy Heat Islands

Cong Wen [1,2,3,4], Ali Mamtimin [1,2,3,4], Jiali Feng [5], Yu Wang [1,2,3,4,*], Fan Yang [1,2,3,4], Wen Huo [1,2,3,4], Chenglong Zhou [1,2,3,4], Rui Li [6], Meiqi Song [1,2,3,4], Jiacheng Gao [1,2,3,4] and Ailiyaer Aihaiti [1,2,3,4]

[1] Institute of Desert Meteorology, China Meteorological Administration, Urumqi 830002, China; wencong@idm.cn (C.W.); ali@idm.cn (A.M.); yangfan@idm.cn (F.Y.); huowenpet@idm.cn (W.H.); zhoucl@idm.cn (C.Z.); songmq@idm.cn (M.S.); gaojiach@idm.cn (J.G.); ailiyaer@idm.cn (A.A.)
[2] Taklimakan Desert Meteorology Field Experiment Station of CMA, Urumqi 830002, China
[3] National Observation and Research Station of Desert Meteorology, Taklimakan Desert of Xinjiang, Urumqi 830002, China
[4] Xinjiang Key Laboratory of Desert Meteorology and Sandstorm, Urumqi 830002, China
[5] Guangdong-Hong Kong-Macao Greater Bay Area Meteorological Monitoring and Warning Forecasting Centre (Shenzhen Institute of Meteorological Innovation), Shenzhen 518000, China; jxf545@gbamwf.com
[6] Suzhou Meteorological Bureau, Suzhou 215100, China; lirui06.23@gmail.com
* Correspondence: wangyu@idm.cn

Abstract: Urban heat islands have garnered significant attention due to their potential impact on human life. Previous studies on urban heat islands have focused on characterizing temporal and spatial variations over longer periods of time. In this study, we investigated the urban heat island (UHI) in Birmingham from September 2013 to August 2014 using higher temporal resolution SEVIRI satellite surface temperature data along with data from the Birmingham Urban Climate Laboratory (BUCL) meteorological station and the UK Meteorological Office meteorological station. Our aim was to characterize the diurnal variations in the surface urban heat island intensity (SUHII) and canopy urban heat island intensity (CUHII) and to explore their relationship under the influence of three factors (day/nighttime, season, and wind speed) using regression analysis. Our findings reveal that SUHII and CUHII exhibit relatively stable patterns at night but vary significantly during the day with opposite diurnal trends. In addition, SUHII and CUHII were more variable in spring and summer but less variable in winter. During the nighttime, SUHII represents CUHII with high confidence, especially during spring and summer, but less so during the cold season. In addition, SUHII represents CUHII with greater confidence under low-wind conditions. This study deepens our understanding of the diurnal dynamics of urban heat islands and the influence of atmospheric conditions on the relationship between surface and canopy heat islands in urban areas. The results of this study can be used for heat island studies in cities that lack high-precision observation networks and to guide sustainable urban development.

Keywords: urban heat islands; canopy urban heat island; diurnal variation

Citation: Wen, C.; Mamtimin, A.; Feng, J.; Wang, Y.; Yang, F.; Huo, W.; Zhou, C.; Li, R.; Song, M.; Gao, J.; et al. Diurnal Variation in Urban Heat Island Intensity in Birmingham: The Relationship between Nocturnal Surface and Canopy Heat Islands. *Land* **2023**, *12*, 2062. https://doi.org/10.3390/land12112062

Academic Editor: Nir Krakauer

Received: 25 September 2023
Revised: 10 November 2023
Accepted: 11 November 2023
Published: 13 November 2023

1. Introduction

In recent years, there has been a growing body of research focusing on the use of satellite data to investigate the temporal and spatial characteristics of urban heat island intensity (UHII) and examine the factors that influence its changes [1–5]. For instance, Feng et al. [6] conducted a study in Xiamen, China, where they utilized a method for quantifying land use trajectories and found a correlation between urbanization and urban heat island phenomena. Their findings showed that changes in land use trajectories and urban heat island intensity are effective measures for evaluating the impact of urbanization on UHII. Another study conducted by Hu and Brunsel [7] in Houston, Texas, employed

MODIS LST products to examine the impact of temporal aggregation on land surface temperature (LST) and surface urban heat islands from 2000 to 2010. The results indicated that SUHII values were higher during the daytime compared to the nighttime. Furthermore, the study revealed that the impact of temporal aggregation on SUHI was more pronounced in the spring and summer compared to the autumn and winter. Similarly, Xu and Liu [8] employed Landsat/TM satellite imagery to derive the near-surface temperature in Beijing, China. The remote sensing data demonstrated significant and distinct urban heat island effects in Beijing, with a clear aggregation pattern and a concentration of intensity in the southern part of the city. Sismanidis et al. [9] examined the diurnal variation in urban heat islands in Athens (GR), Istanbul (TR), and Rome (IT) during the summer of 2014 using LST data from the National Astronomical Observatory of Athens (NOA/IAASASRS). The study revealed a strong SUHII effect in all three cities during both noon and nighttime. However, despite being situated in the same climate zone, each city exhibited unique characteristics in terms of SUHII. Anniballe et al. [10] utilized data from the Moderate Resolution Imaging Spectrometer (MODIS) satellites to generate a map of the urban heat island in Milan, Italy. They analyzed both CUHII and SUHII. The study found that during the summer, SUHII exhibited stronger activity during the day but decreased at night. Notably, there was no canopy heat island during the day, which only appeared after sunset. Comparing UHII with the normalized vegetation index (NDVI) confirmed that high vegetation coverage can mitigate urban heat islands. In a study conducted in Ahmedabad and Jaipur, India, remote sensing data from the MODIS sensors were employed to investigate the urban heat island effect during both the day and night [11]. The results revealed higher temperatures during the day, but urban heat islands were primarily observed at night. Moreover, a reversal of SUHII was observed during the day, with clear SUHII observed at night. These studies highlight the value of satellite data in understanding the dynamic nature of urban heat islands as well as the influence of various factors on their intensity.

With the rapid development of the satellite field, more and more satellite data can provide surface temperature parameters. Table 1 summarizes the characteristics of commonly used satellite sensors for surface temperature, such as time and spatial resolution. When researching, the appropriate satellite data should be selected based on their own characteristics and the research needs. From this, we can find that a Spinning Enhanced Visible and Infrared Imager (SEVIRI) high temporal resolution has many advantages, which provide the possibility for studying the daily changes in SUHII. Tomlinson et al. [12] reviewed satellites, sensors, and studies related to ground-based temperature measurements and noted that SEVIRI has the potential to study LST models during daytime hours. Zakšek et al. [13] used SEVIRI data to study SUHII with high temporal resolution and obtained data that facilitated the analysis of UHI diurnal variability. These previous studies provide a preliminary basis for this study.

Table 1. The characteristics of commonly used satellite sensors for surface temperature.

Sensor	Satellite	Spatial Resolution	Time Resolution	Website
Landsat ETM+	Landsat 7	60 m	16 days	https://landsat.gsfc.nasa.gov/etm-plus/, accessed on 10 May 2023
TIRS	Landsat 8	100 m	16 days	https://landsat.gsfc.nasa.gov/satellites/landsat-8/landsat-8-mission-details/, accessed on 10 May 2023
MODIS	Aqua	~1 km	Twice daily	https://modis.gsfc.nasa.gov/data/dataprod/mod11.php, accessed on 10 May 2023
MODIS	Terra	~1 km	Twice daily	https://modis.gsfc.nasa.gov/data/dataprod/mod11.php, accessed on 10 May 2023
AVHRR	Multiple NOAA	~1.1 km	Twice daily	https://www.eumetsat.int/avhrr, accessed on 10 May 2023
VIIRS	JPSS	~400 m	Every 4 h	https://www.star.nesdis.noaa.gov/jpss/VIIRS.php, accessed on 10 May 2023

Table 1. *Cont.*

Sensor	Satellite	Spatial Resolution	Time Resolution	Website
ABI	GOES-R	~2 km	Every 15 min	https://www.goes-r.gov, accessed on 10 May 2023
SEVIRI	Meteosat-8	~3 km	Every 15 min	https://landsaf.ipma.pt/en/data/products/land-surface-temperature-and-emissivity/, accessed on 10 May 2023

Urban heat islands are a well-known phenomenon, encompassing various layers such as the subsurface layer heat island, the surface layer heat island, the canopy layer heat island, and the boundary layer heat island (BUHI) [14]. Previous studies have examined the characteristics and distribution of these different types of urban heat islands. In recent years, researchers have also focused on investigating the relationship between the surface heat island intensity and the canopy heat island intensity [15]. While satellite data are commonly used to obtain SUHI information, CUHII data are often derived from observations at weather stations. Consequently, researchers have utilized different satellite data to explore the relationship between SUHII and CUHII, aiming to identify the factors that influence this relationship. For instance, Feng et al. [16] examined the SUHII–CUHII relationship in Birmingham, UK, considering factors such as season, wind speed (WS), and land use categories modified according to the local climate zone. They found that satellite data can provide reliable estimates of CUHII, particularly under low WS conditions. In another study, Ioannis et al. [17] investigated the urban heat island effect in the Athens metropolitan area, combining ground observations with spacecraft remote sensing. Walawender et al. [18] compared different satellite data and surface temperature retrieval algorithms in Krakow, Poland, to evaluate their advantages and disadvantages. Fabrizi et al. [19] analyzed Rome's urban heat island trend using ground weather stations and satellite infrared sensors, demonstrating the usefulness of satellite data for CUHII retrieval. Pandey et al. [20] utilized MODIS satellite data to analyze the urban heat island phenomenon in Delhi during both day and night. Their findings confirmed the presence of urban heat islands in Delhi at night and highlighted the role of urban areas as regulators of temperature changes under low-wind conditions. Furthermore, Feng et al. [21] compared the SUHII–CUHII relationship under different weather conditions in Oklahoma City, USA, and Birmingham, UK, using MODIS data and the Urban Weather Network. They also compared the canopy urban heat island and surface urban heat island of Beijing, China, based on MODIS data, considering the spatial scale of the city. The comparison revealed that CUHII exhibited good agreement with SUHI at night, but during the daytime, both the intensity and spatial distribution of the heat island differed significantly. Additionally, the intensity difference between SUHII and CUHII showed distinct seasonal changes during the day, being small and negative in the cold season and large and positive in the warm season, while no significant seasonal change was observed at night [14].

Through an investigation of the relevant literature, it was found that a large number of studies have used satellite data with low time resolution and focused on the temporal and spatial distributions of urban heat islands over longer time scales. There are also some studies focusing on the relationship between SUHII and CUHII and exploring its influencing factors. However, there are few studies using high time resolution data to explore the diurnal characteristics of urban heat islands and the relationship between SUHII and CUHII. Therefore, this study uses SEVIRI satellite data with a time resolution of 15 min combined with meteorological data to explore the diurnal characteristics of the Birmingham urban heat island and examine the relationship between SUHII and CUHII.

2. Materials and Methods

2.1. Study Area

Birmingham (52.5° N,1.9° W) is a large industrial city located in the West Midlands, England. Birmingham covers an area of approximately 278 km^2 and is the second-largest city in the UK. According to statistics, in 2013, Birmingham had a population of approximately 1,092,330 [22]. Birmingham has a temperate maritime climate, with warm winters and cool summers, rainy seasons throughout the year, and more rainfall in winter. Figure 1 shows the geographic location of Birmingham and weather stations. The Urban Atlas land use type is derived from the European Environment Agency (EEA).

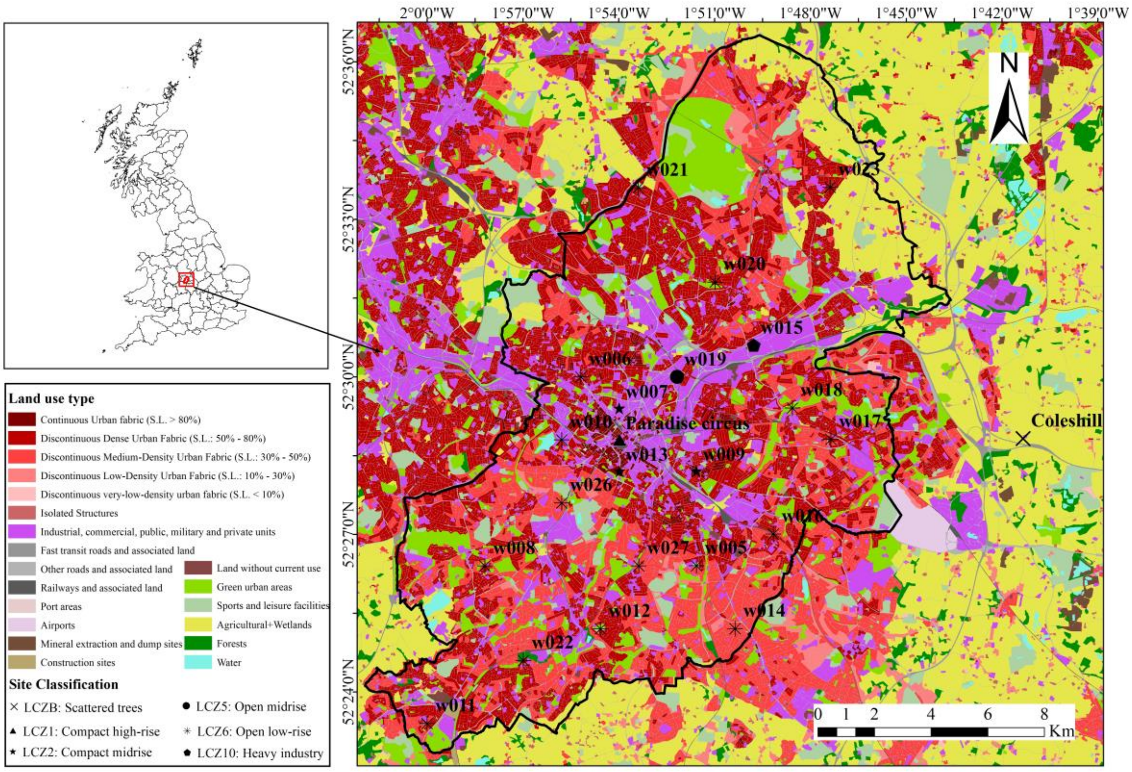

Figure 1. Birmingham city weather station location.

2.2. *Meteorological Data*

The Birmingham Urban Climate Laboratory (BUCL), established in the UK, is a high-density urban weather network of automatic weather stations [23]. BUCL installed 25 automatic weather stations in Birmingham, which recorded temperature, relative humidity, atmospheric pressure, wind speed and direction, and precipitation 3 m above the ground. Bassett et al. [24] summarized the specific locations of 25 BUCL weather observation stations and the local climate zone (LCZ) in which they are located [25]. However, due to equipment and other reasons, there are data missing at individual meteorological stations during the time period selected in this study. This study uses data from 20 Vaisala WXT520 stations in the urban area that have observational data during the study period. In addition, this study also incorporates data from two weather stations operated by the British Met Office, namely, Paradise Circus and Coleshill Station, to complement the site-specific measurements. Paradise Circus is situated in the central area of the city, whereas Coleshill Station is positioned outside the urban region. Utilizing data from these two stations proves highly advantageous for studying the urban heat island (UHI) phenomenon due to their strategic locations [16]. In our analysis, Coleshill station can be used as a rural reference station. The data used in this study are data from 20 BUCL city stations and 2 UK Met Office weather stations from August 2013 to August 2014. This period of time was chosen because of the availability and convenience of the data, in contrast to previous studies.

2.3. Site Classification

The local climate zone (LCZ) is one of the most important indicators for urban-heat-island-related studies. The LCZ defines the nature of urban climate, air quality, and temperature at the local level. In the study of heat island effects, the division of station LCZ will directly affect the calculation of heat island intensity. Based on a previous study [25] of surface temperature in the Birmingham area, the BUCL site was divided into five different LCZs (Figure 1). In this study, the LCZs were utilized to divide the observation sites into urban and suburban.

2.4. Satellite Data

2.4.1. SEVIRI Satellite

The Surface Analysis Satellite Application Facility (SAF) is part of the SAF network, which is a dedicated development and processing center and is the ground part of EUMETSAT (European Meteorological Satellite Development Organization) distributed applications [26]. The main purpose of Land Surface Analysis (LSA) SAF is to make full use of remote sensing data (especially data obtained from EUMETSAT sensors) to measure land surface variables. These variables are used for the meteorology spin-stabilized Meososat second-generation (MSG) imaging repetition period, which is 15 min long. However, LSA SAF has great potential to contribute to weather forecasting and climate modeling, environmental management and land use, agricultural and forestry applications, natural disaster management, climate applications, and climate change detection.

The satellite data selected in this study come from SEVIRI's land surface temperature (LST) data. SEVIRI is the main instrument of the Meteosat second-generation (MSG) satellite system, which can provide accurate meteorological data about sea and land temperature, cloud cover, etc. MSG has twelve spectral channels, eight of which are located in the thermal infrared channel. SEVIRI can provide satellite images [27] with a spatial resolution of 3 km every 15 min. SEVIRI LST data use the general split window (GSW) algorithm [28]. GSW corrects atmospheric data based on the absorption differences of adjacent IR bands. In theory, SEVIRI can provide 96 images per day, but due to factors such as cloud cover, the actual available data number is far less than 96. The generalized split window (GSW) algorithm is a semi-empirical algorithm that allows the estimation of LST from top-of-atmosphere brightness temperatures of two adjacent channels within the atmospheric window part of the spectrum, assuming the channel surface is known [28]. The main error sources of SEVIRI LST include the following: the uncertainty of the GSW algorithm itself and the systematic error of surface emissivity.

SEVIRI LST data cover Europe. The data format for the three major geographic regions of North Africa, South Africa, and South America is hdf5. The data sets contain information on the following: the general attribute set of various data, the data set of parameter values, and the data set of error values and quality flags. The data set used in this study is for Europe. The European data set has 651 rows, 1701 columns, and a total of 1107.351 pixels.

To verify the availability of SEVIRI data in the Birmingham area, we selected 3 September 2013, a day with low cloudiness, and calculated the diurnal variation in the station mean temperature using BUCL observations, SEVIRI LST data, and MODIS LST. From Figure 2, we can see that the SEVIRI LST data are similar to the observed data in terms of nocturnal trends, although there are some missing measurements at individual times. The difference with the MODIS LST data is relatively small. For further verification, we selected the days with cloudiness below 4 from August 2013 to August 2014 to correlate the SEVIRI LST data with the BUCL observations (Figure 3), and it can be concluded that they have a high correlation. Thus, the SEVIRI LST data are available in the Birmingham area.

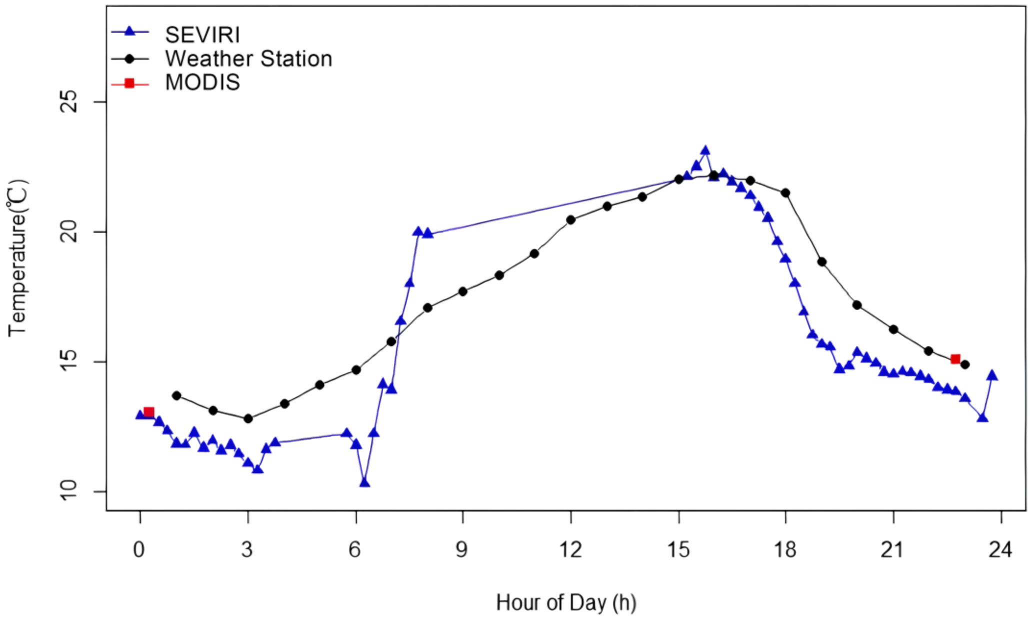

Figure 2. Diurnal variations in SEVIRI LST, MODIS LST, and air temperature at BUCL on 3 September 2013.

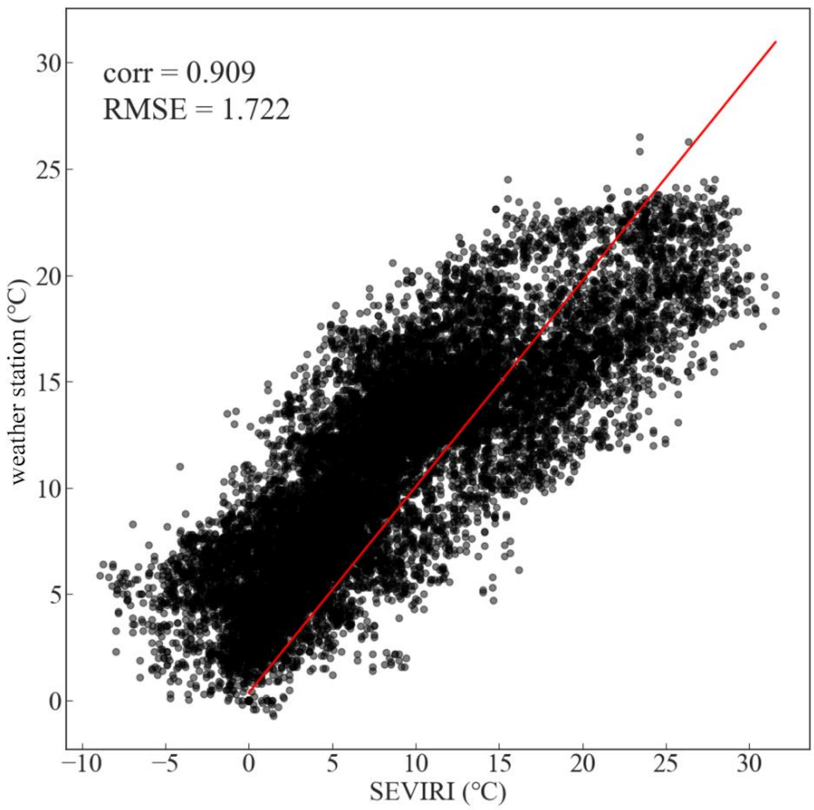

Figure 3. Correlation analysis of SEVIRI LST data with BUCL observation data.

2.4.2. Temporal and Spatial Consistency

The data used in this study come from the following two parts: one is the surface temperature data Ts from SEVIRI, and the other is the canopy temperature data Ta from the weather station. The time accuracy of SEVIRI LST is 15 min. The time accuracy of the weather station data is hourly. Therefore, in this study, the average of the four Ts values within one hour is selected to represent the hourly value of Ts so as to ensure the temporal consistency between Ts and Ta. Because the data type of Ta is point data, the data type of Ts is pixel data. Therefore, in order to ensure spatial consistency between Ts and Ta, in this study, the pixel point where the weather station is located can be located according to the latitude and longitude data of the weather station, and the temperature value of the pixel point is used to represent the Ts of the weather station.

2.5. Estimation of UHII

According to the definition of urban heat islands, *UHII* is the temperature difference between urban and rural areas.

$$SUHII = T_S^U - T_S^R \tag{1}$$

$$CUHII = T_C^U - T_C^R \tag{2}$$

Here, *U* represents urban, and *R* represents rural. In this study, we chose Coleshill station to represent the rural area. We selected 20 BUCL stations and 1 station from the Meteorological Bureau to represent the urban area. For the estimation of *SUHII*, we selected the average of the pixels of these 21 stations to represent the urban surface temperature (T_S^U), which is the temperature of the air near the surface of the earth. For the estimation of *CUHII*, we selected the average temperature of these 21 stations to represent the urban canopy temperature (T_C^U), which is the temperature of plants and the vegetative cover.

2.6. Statistic Method

This study grouped all the station data according to day/nighttime, season, and wind speed to further explore the relationship between SUHII and CUHII under different conditions. A linear regression model was also used to explain the relationship between SUHII and CUHII, and significance tests were performed at the 0.01 significance level. In this study, the confidence ellipse generated at the 90% confidence level was used for two-dimensional distribution analysis, and this step added the analysis of the relationship between the two variables, such as the mean and standard deviation. The value of the x-y coordinate in the center of the confidence ellipse is the mean of the two variables, SUHII and CUHII. The size of the confidence ellipse is the eigenvalue of the covariance matrix, and the direction of the confidence ellipse is the eigenvector of the size of the confidence ellipse.

3. Results

3.1. Diurnal Variation in SUHII

Using SEVIRI data from August 2013 to August 2014, we examined the daily variability characteristics of SUHII in Birmingham's urban core and suburban areas over the course of a year. From Figure 4a, it can be seen that SUHII varied considerably over the diurnal cycle, particularly in the urban core. Both in the urban core and in the suburbs, SUHII showed clear daily variability, with SUHII being stronger during the day than at night. Moreover, urban core and suburban areas demonstrated a similar pattern in their daily variation, i.e., higher SUHII during the day when solar radiation was stronger and less variation in SUHII during the night. In terms of overall SUHII, urban areas were higher than suburban areas. During the day, the peak of SUHII in both the urban core and suburban areas occurred at 13:00 noon, and the lowest value occurred at 5:00 a.m. The difference was that the highest SUHII value in the urban area was 4 °C, and the lowest value was 0.5 °C. The peak SUHII value in the suburban area was 2.5 °C, and the lowest value was 0.3 °C.

In order to further investigate the variation in the SUHII daily characteristics based on the seasons, we divided SUHII into four seasons, spring, summer, autumn, and winter, according to the meteorological definition of seasons (Figure 4). In the four seasons, SUHII in the urban region had a similar trend to that in the suburban region, i.e., it fluctuated more during the day and reached its maximum value during the day at midday. The ranges of SUHII in the urban region during the four seasons were 1.2–6, 1.1–7, 1.1–3.5, and 0.7–1.8. The ranges of SUHII in the suburban region during the four seasons were 1–6, 1.1–4, 1.1–2, and 0.7–2, respectively. It is worth noting that the daily variation characteristics were strongly seasonal in the daytime variation characteristics, while the nighttime variation characteristics were more similar in different seasons. In the summer, the variability in SUHII was greater. In winter, the variability in SUHII was smaller. Therefore, the difference between SUHII in urban and suburban areas was smaller in the winter.

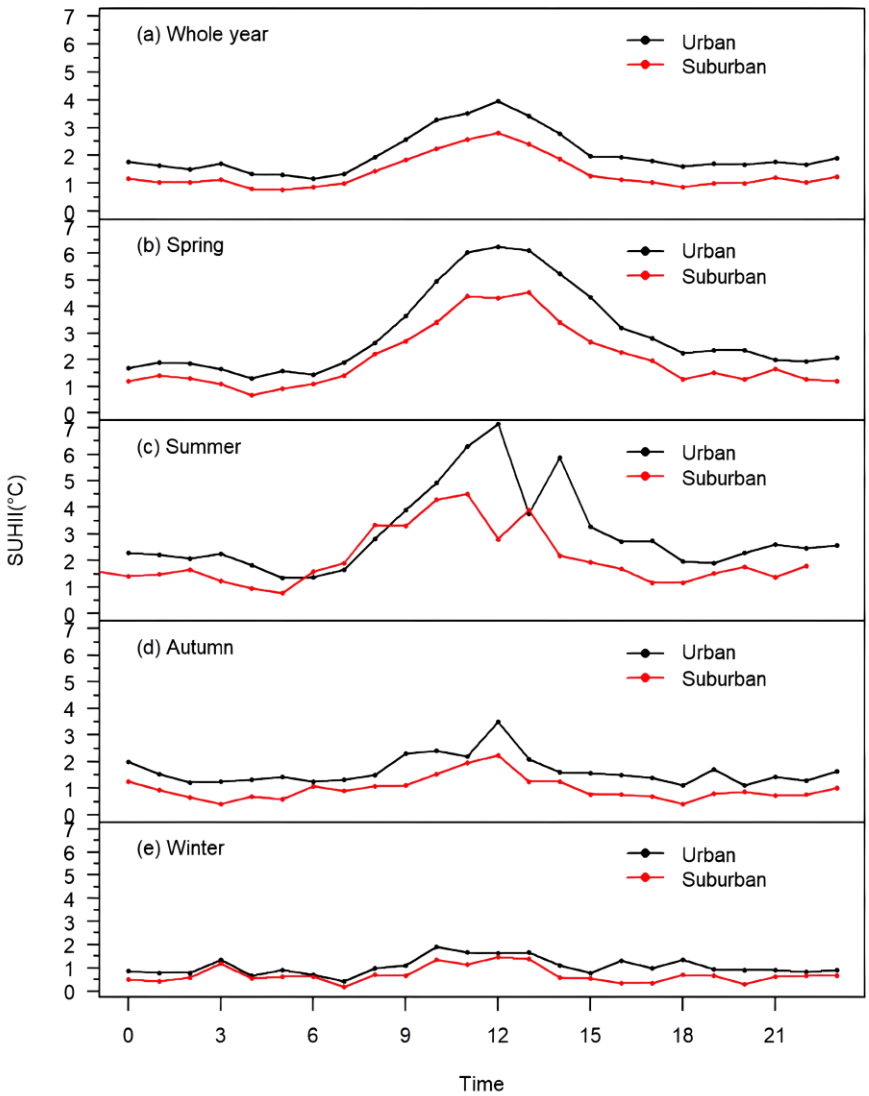

Figure 4. Diurnal variation in SUHII throughout the year.

3.2. Diurnal Variation in CUHII

We investigated the daily variation characteristics of CUHII in urban and suburban areas using observations from weather stations. As shown in Figure 5a, CUHII shows a clear daily variation. In the daily variation, CUHII is higher at night than CUHII during the day. CUHII in urban and suburban areas has the same trend during the daytime; however, CUHII in urban areas is greater than CUHII in suburban areas. CUHII reached its lowest value at 13:00 noon in both urban and suburban areas, and it reached its highest value during the day at 3:00 a.m. The difference is that the range of CUHII in the urban region is 0.19 to 0.93, and the range of CUHII in the suburban region is −0.36 to 0.44.

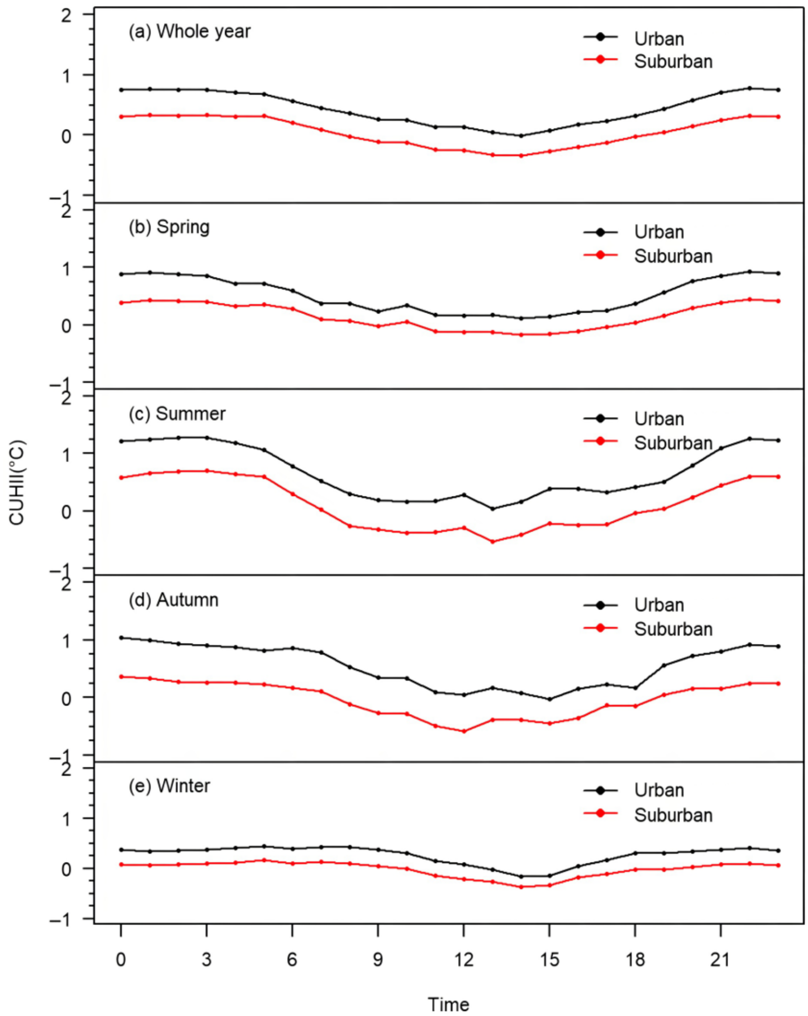

Figure 5. Diurnal variation in CUHII throughout the year.

We further analyzed the daily variation characteristics of CUHII in the four seasons (Figure 5). In the four seasons, CUHII in both urban and suburban regions showed obvious seasonal variations, and the daily variation trends were consistent. The ranges of CUHII in the urban region in spring, summer, autumn, and winter were 0.11–0.93, 0.05–1.28, −0.03–1.05, and −0.17–0.44, respectively. The ranges of CUHII in the suburban region in the spring, summer, autumn, and winter seasons were −0.18–0.45, −0.53–0.71, −0.58–0.37, and −0.37–0.17. The variation in CUHII in winter was more moderate, and the variation in CUHII in summer was larger. In winter, the difference between CUHII in the urban area and the suburban area was smaller.

3.3. Difference between SUHII and CUHII in the Daytime and Nighttime

When we studied the daily variation in SUHII and CUHII, we found that SUHII and CUHII had a large variation trend during the day, but they were more similar at night. SUHII and CUHII data from all stations were grouped as daytime and nighttime. The linear regressions and 2D distributions between SUHII and CUHII are outlined in Figure 6. We are more confident in estimating CUHII based on SUHII during the nighttime. Therefore, in a subsequent study, we will investigate the relationship between SUHII and CUHII at night.

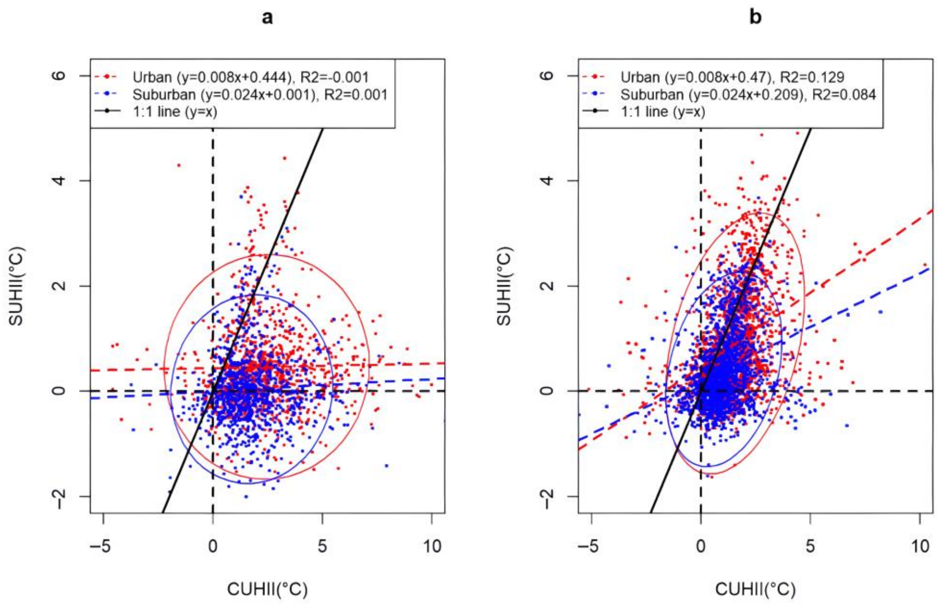

Figure 6. Linear and elliptical trends of SUHII and CUHII based on the daytime and nighttime: (**a**) daytime; (**b**) nighttime.

3.4. The Effect of Wind

All nighttime data were classified as WS1 (WS < 2 m/s), WS2 (WS = 2–4 m/s), and WS3 (WS = 4–6 m/s), according to three different wind speed conditions. From Figure 7, it can be observed that the mean values of SUHII and CUHII decrease with increasing WS according to the estimated trend of the ellipse center moving toward (0,0). Under low-wind-speed conditions, we are more confident in estimating CUHII based on SUHII.

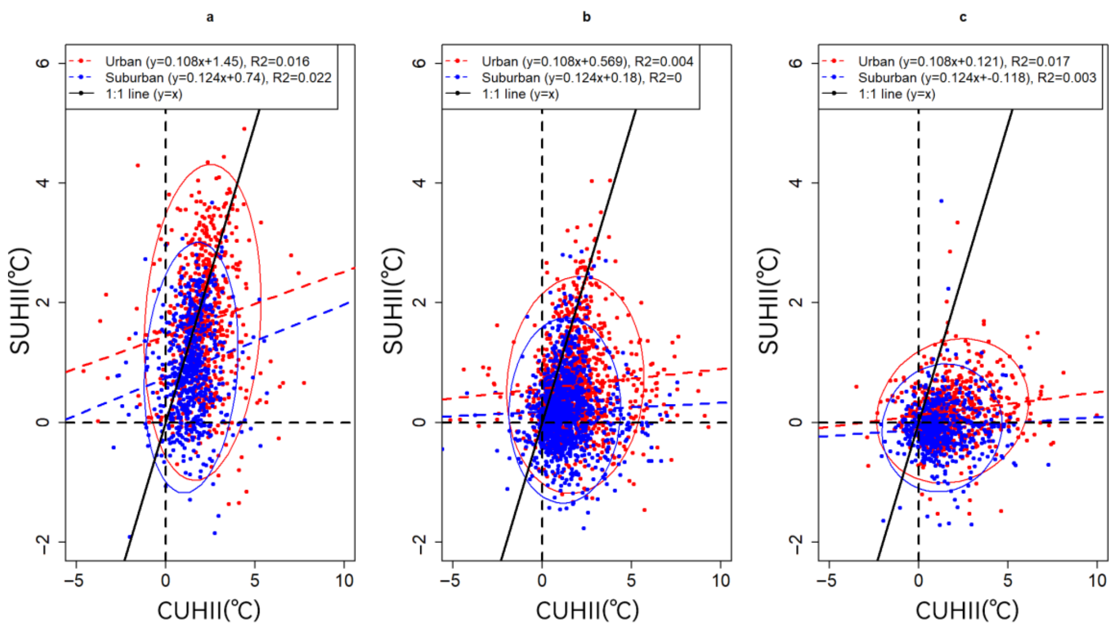

Figure 7. Linear and elliptical trends of SUHII and CUHII based on three wind speed conditions: (**a**) WS1, (**b**) WS2, and (**c**) WS3.

3.5. Seasonal Difference

In Figure 8, a summary of the linear regression models estimated in the nighttime for the four seasons is shown. Among the different seasons, the higher R^2 values in the spring and summer indicate that SUHII responds better to CUHII in the spring and summer, and the lower R^2 values in the fall and winter indicate that there are more uncertainties affecting the SUHII–CUHII relationship. The limited sample size in fall and winter due to fewer clear nights is also a potential factor for lower R^2. In colder seasons, the magnitudes of SUHII and CUHII are smaller, leading to lower confidence in the estimated linear regression model. In addition, stronger anthropogenic heat (especially from space heating) may account for the lower data correlation between SUHII and CUHII, which also contributes to the lower R^2 values.

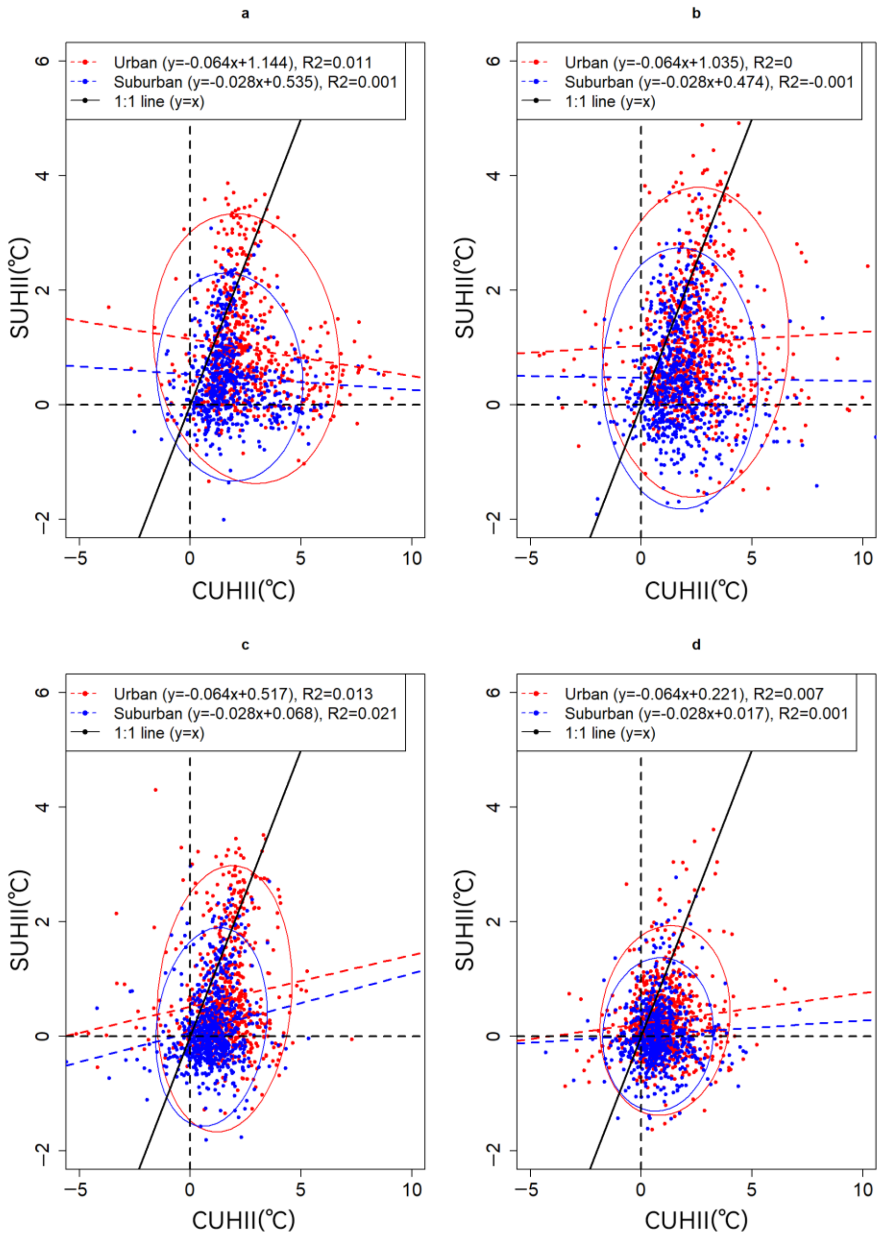

Figure 8. Linear and elliptical trends of SUHII and CUHII based on the season: (**a**) spring, (**b**) summer, (**c**) autumn, and (**d**) winter.

4. Discussion

As a widely concerned issue in urban climatology and urban planning, many scholars have already studied urban heat islands using satellite data. In other studies, MODIS LST data were selected to study urban heat islands [29–31]. However, canopy temperatures have some advantages for studying urban heat islands. Fortunately, the establishment of some urban meteorological observation networks provides research conditions for this purpose. The relationship between urban surface temperature and canopy temperature has been studied using high-density urban meteorological network data in comparison with MODIS LST [32]. However, due to the limitation of temporal resolution, MODIS only provides two sets of data per day, so there is a certain gap in the study of daily changes in urban heat islands using satellites. According to the literature, very few studies have utilized geostationary satellites to study the daily variation in SUHII. In this study, the daily variation characteristics of SUHII and CUHII in Birmingham are investigated using high temporal resolution SEVIRI LST data and weather station data, and the relationship between SUHII and CUHII under different conditions is explored. This provides a possibility to study the formation mechanism of SUHII. Moreover, this study can provide a reference for urban heat island studies in cities that lack urban meteorological observation networks, with a view to help urban planning and construction.

In our study, we found that SUHI shows significant daily variability in the urban core and suburban areas, with higher SUHII during the daytime when solar radiation is stronger and less variability in SUHII at night. This study attempts to provide some explanations for such phenomena. In general, the LCZ in rural areas is different from that in cities. The land cover type in rural areas is mainly soil and vegetation, while the land cover in cities is mainly impermeable concrete. Urban soil cover types have a relatively high heat absorption capacity and poor ventilation in cities, while rural areas are relatively open, and the soil and vegetation at the surface absorb heat slowly. Solar radiation increases in the afternoon, and as a result, SUHII peaks at 13:00 p.m. At 5:00 a.m., the soil has largely released the heat absorbed the previous day, and the heat absorption process has not yet started, so the lowest temperature occurs. Seasonal differences in SUHII are influenced via conditions such as sunshine intensity, sunshine duration, and soil moisture [33].

By comparing the diurnal trends of CUHII in different periods, we observed some common characteristics of CUHII throughout the year and in different seasons: CUHII shows significant daily variations. In the urban region, in spring, summer, autumn, and winter, they were 0.11–0.93, 0.05–1.28, −0.03–1.05, and −0.17–0.44, respectively. The ranges of CUHII in the suburban region in the spring, summer, autumn, and winter seasons were −0.18–0.45, −0.53–0.71, −0.58–0.37, and −0.37–0.17, respectively. CUHII is higher at night than CUHII during the day, and the diurnal trend of CUHII had a "V" shape throughout the year and in all seasons. Compared with SUHII, CUHII was smaller [32]. CUHII is always higher in the urban core than in the suburban areas.

Comparing the diurnal characteristics of CUHII and SUHII, we can find that the differences in CUHII and SUHII are relatively flat at night and more drastic during the daytime over the whole year and across all seasons. However, the difference is that SUHII peaks during the day and CUHII reaches its low value during the day. The studies by Pandey et al. [20] and Chang et al. [34] showed the same characteristics. However, CUHII and SUHII have large diurnal variations in spring and summer but less diurnal variation in winter. The diurnal ranges of CUHII in spring were 0.11–0.93 and −0.18–0.45 in urban and suburban areas, respectively; 0.05–0.28 and −0.53–0.71 in summer, respectively; and −0.17–0.44 and −0.37–0.17 in winter, respectively. The diurnal ranges of SUHII in spring were 1.2–6 and 1–6 in urban and suburban areas, respectively; 1.1–7 and 1.1–4 in summer, respectively; and 0.7–1.8 and 0.7–2 in winter, respectively. This phenomenon has been confirmed by many previous studies [35,36]. The thermal conductivity of land cover type, sunshine duration, and soil moisture are the main reasons for this phenomenon.

A seasonal analysis of diurnal variation in SUHII was conducted to understand how this phenomenon varies across seasons. Seasonal variations can have a significant impact on the urban heat island effect, as various factors such as solar radiation, vegetation cover, cloud cover, and meteorological conditions may vary from season to season. In addition, a study by Fortuniak et al. in Central Europe showed favorable UHI at night in summer due to clear weather and strong winds [37]. Zhou et al. showed that the seasonality of soil moisture was related to UHI in London, so the dryness of the summer months in the Birmingham area may have an impact on SUHII [38]. The linear and elliptical trends of SUHII and CUHII based on three wind speed conditions may be related to wind advection.

The spatial pattern of CUHII is altered by advection due to the wind-directed transport of air temperature. The spatial pattern of SUHII should be more influenced by local-scale radiative processes and less by advection. In addition, higher WS tends to disrupt the nocturnal stabilization layer over rural surfaces and bring warmer air aloft, increasing temperatures there and, thus, reducing the intensity of CUHII. Although this process may also raise temperatures in rural areas, the magnitude of the CUHII reduction is likely to be smaller.

High-resolution geostationary satellites show great potential for studying the daily changes in urban heat islands and for urban spatial planning. However, due to cloudiness, SEVIRI provides less available data in winter, which can have an impact on the analysis of the results. Additionally, due to the lower spatial resolution of geostationary satellites, they are only suitable for application in some larger cities. The urban thermal environment is a factor that should not be neglected in the process of urban planning, and different land use types and human activities will have an impact on the surface temperature [39]. AlDousari et al. used Landsat images to study the effect of land use and land cover type replacement on thermal comfort zones and found that the increase in urban areas was accompanied by an increase in thermal comfort zones [40]. The increase in built-up areas will change the pattern of SUHII [41]. Therefore, the retention of green spaces should be considered in future urban planning [42,43] to ensure the sustainable development of cities.

5. Conclusions

In this study, we utilized high temporal resolution SEVIRI satellite data and observatory site data to investigate the variation characteristics of SUHII and CUHII in the Birmingham area as well as the relationship between SUHII and CUHII under the influence of different factors. Our conclusions are as follows:

(A). SUHII and CUHII have distinctive daily variation characteristics that are relatively stable at night but vary drastically during the day, with opposite diurnal trends. (B). The daily variation characteristics of SUHII and CUHII show similar patterns in the four seasons. (C). The heat island intensity is stronger in the urban core than in the suburbs. (D). At night, SUHII is more representative of CUHII. (E). In the spring and summer, SUHII is more representative of CUHII but less representative in the cold season. (F). The confidence in estimating CUHII with SUHII is higher under low-wind conditions. Using the new SEVIRI data, this study provides the daily variation characteristics of the urban heat island, which fills the gap of other satellites with lower temporal resolution and helps to explain the physical process of the urban heat island during the day/night. In addition, this study investigates the relationship between SUHII and CUHII, which provides a reference basis for cities that lack a dense urban observation network and is beneficial to heat island research and sustainable urban development.

However, this study has some limitations. First, the SEVIRI LST satellite data have some deficiencies due to cloud cover, which greatly reduces the average representativeness of the LST data for some time periods. Second, due to the low spatial resolution of SEVIRI, some weather stations are at the same pixel point in the LST data. In future studies, the SEVIRI satellite data could be downscaled to improve the spatial resolution of the data. The increased use of other satellite data for comparison is also a good approach. The use of satellite data with longer durations could make LST data more reliable over time and increase the possibility of inter-annual comparisons.

Author Contributions: Conceptualization, C.W. and A.M.; methodology, C.W. and J.F.; data curation, Y.W. and R.L.; writing—original draft preparation; writing—review and editing, M.S., A.A. and J.G.; visualization, C.W. and F.Y.; supervision, W.H. and C.Z.; funding, A.M. All authors have read and agreed to the published version of the manuscript.

Funding: This research was funded by the China Desert Meteorology Research Foundation (Grant number: Sqj2021005 and Sqj2022001), the Xinjiang Key Laboratory of Desert Meteorology and Sandstorms Award Funding (Grant number: 2023-38), the Xinjiang Meteorological Bureau Science and Technology Innovation Development Fund Project (Grant number: MS202309 and MS202312) the Scientific, Technological Innovation Team (Tianshan Innovation Team) project (Grant number: 2022TSYCTD0007), and the National Natural Science Foundation of China (Grant number: 42205088).

Data Availability Statement: Data used in this study can be provided by Congwen (wencong@idm.cn) upon request.

Acknowledgments: We are grateful to BUCL and EUMETSAT for providing data support.

Conflicts of Interest: The authors declare no conflict of interest.

References

1. Grimm, N.B.; Faeth, S.H.; Golubiewski, N.E.; Redman, C.L.; Wu, J.; Bai, X.; Briggs, J.M. Global change and the ecology of cities. *Science* **2008**, *319*, 756–760. [CrossRef] [PubMed]
2. Howard, L. *The Climate of London, Deduced from Meteorological Observations, Made at Different Places in the Neighbourhood of the Metropolis*; W. Phillips: London, UK, 1818; Volume I.
3. Buyantuyev, A.; Wu, J. Urban heat islands and landscape heterogeneity: Linking spatiotemporal variations in surface temperatures to land-cover and socioeconomic patterns. *Landsc. Ecol.* **2010**, *25*, 17–33. [CrossRef]
4. Bornstein, R.D. Observations of the Urban Heat Island Effect in New York City. *J. Appl. Meteorol. Climatol.* **1968**, *7*, 575–582. [CrossRef]
5. Heaviside, C.; Vardoulakis, S.; Cai, X.M. Attribution of mortality to the urban heat island during heatwaves in the West Midlands, UK. *Environ. Health* **2016**, *15*, 49–59. [CrossRef]
6. Feng, H.; Zhao, X.; Chen, F.; Wu, L. Using land use change trajectories to quantify the effects of urbanization on urban heat island. *Adv. Space Res.* **2014**, *53*, 463–473. [CrossRef]
7. Hu, L.; Brunsell, N.A. The impact of temporal aggregation of land surface temperature data for surface urban heat island (SUHI) monitoring. *Remote Sens. Environ.* **2013**, *134*, 162–174. [CrossRef]
8. Xu, Y.; Liu, Y. Monitoring the Near-surface Urban Heat Island in Beijing, China by Satellite Remote Sensing. *Geogr. Res. J. Inst. Aust. Geogr.* **2015**, *53*, 16–25. [CrossRef]
9. Sismanidis, P.; Keramitsoglou, I.; Kiranoudis, C.T. Diurnal analysis of surface Urban Heat Island using spatially enhanced satellite derived LST data. In Proceedings of the 2015 Joint Urban Remote Sensing Event (JURSE), Lausanne, Switzerland, 30 March–1 April 2015. [CrossRef]
10. Anniballe, R.; Bonafoni, S.; Pichierri, M. Spatial and temporal trends of the surface and air heat island over Milan using MODIS data. *Remote Sens. Environ.* **2014**, *150*, 163–171. [CrossRef]
11. Mathew, A.; Khandelwal, S.; Kaul, N. Analysis of diurnal surface temperature variations for the assessment of surface urban heat island effect over Indian cities. *Energy Build.* **2017**, *159*, 271–295. [CrossRef]
12. Tomlinson, C.J.; Chapman, L.; Thornes, J.E.; Baker, C. Remote sensing land surface temperature for meteorology and climatology: A review. *Meteorol. Appl.* **2011**, *18*, 296–306. [CrossRef]
13. Zakšek, K.; Oštir, K. Downscaling land surface temperature for urban heat island diurnal cycle analysis. *Remote. Sens. Environ.* **2011**, *117*, 114–124. [CrossRef]
14. Chen, Y.; Sun, H.; Li, J. Estimating daily maximum air temperature with MODIS data and a daytime temperature variation model in Beijing urban area. *Remote Sens. Lett.* **2016**, *7*, 865–874. [CrossRef]
15. Lai, J.; Zhan, W.; Voogt, J.; Quan, J.; Huang, F.; Zhou, J.; Bechtel, B.; Hu, L.; Wang, K.; Cao, C.; et al. Meteorological controls on daily variations of nighttime surface urban heat islands. *Remote Sens. Environ.* **2020**, *253*, 112198. [CrossRef]
16. Feng, J.; Cai, X.; Chapman, L. Impact of atmospheric conditions and levels of urbanisation on the relationship between nocturnal surface and urban canopy heat islands. *Q. J. R. Meteorol. Soc.* **2019**, *145*, 3284–3299. [CrossRef]
17. Daglis, I.A.; Rapsomanikis, S.; Kourtidis, K.; Melas, D.; Papayannis, A.; Keramitsoglou, I.; Giannaros, T.; Amiridi, V.; Petropoulos, G.; Georgoulias, A.; et al. Results of the DUE Thermopolis Campaign with Regard to the Urban Heat Island (UHI) Effect in Athens. *Differ. Equ.* **2007**, *43*, 299–310. [CrossRef]
18. Walawender, J.P. Wykorzystanie danych satelitarnych landsat i technik gis w badaniach warunków termicznych miasta (na przykładzie aglomeracji krakowskiej)/Application of LANDSAT satellite data and GIS techniques for estimation of thermal conditions in urban area (using an example of Kraków agglomeration). *Pr. Geogr.* **2009**, *122*, 81–98.
19. Roberto, F.; Stefania, B.; Riccardo, B. Satellite and Ground-Based Sensors for the Urban Heat Island Analysis in the City of Rome. *Remote Sens.* **2010**, *2*, 1400–1415. [CrossRef]
20. Pandey, P.; Kumar, D.; Prakash, A.; Masih, J.; Singh, M.; Kumar, S.; Jain, V.K.; Kumar, K. A study of urban heat island and its association with particulate matter during winter months over Delhi. *Sci. Total Environ.* **2012**, *414*, 494–507. [CrossRef]
21. Feng, J.; Cai, X.; Chapman, L. A tale of two cities: The influence of urban meteorological network design on the nocturnal surface versus canopy heat island relationship in Oklahoma City, US and Birmingham, UK. *Int. J. Climatol.* **2020**, *41*, E445–E462. [CrossRef]

22. Birmingham City Council. 2011 Birmingham Population & Migration Topic Report. 2013. Available online: https://www.birmingham.gov.uk/downloads/file/9742/2011_birmingham_population_and_migration_topic_report (accessed on 7 April 2023).
23. Chapman, L.; Muller, C.L.; Young, D.T.; Warren, E.L.; Grimmond, C.S.B.; Cai, X.-M.; Ferranti, E.J.S. The Birmingham Urban Climate Laboratory: An Open Meteorological Test Bed and Challenges of the Smart City. *Bull. Am. Meteorol. Soc.* **2015**, *96*, 197–210. [CrossRef]
24. Bassett, R.; Cai, X.; Chapman, L.; Heaviside, C.; Thornes, J.E.; Muller, C.L.; Young, D.T.; Warren, E.L. Observations of urban heat island advection from a high-density monitoring network. *Q. J. R. Meteorol. Soc.* **2016**, *142*, 2434–2441. [CrossRef]
25. Warren, E.L.; Young, D.T.; Chapman, L.; Muller, C.; Grimmond, C.; Cai, X.-M. The Birmingham Urban Climate Laboratory—A high density, urban meteorological dataset, from 2012–2014. *Sci. Data* **2016**, *3*, 160038. [CrossRef] [PubMed]
26. EUMETSAT LSA SAF Product User ManualLand Surface Temperature (LST). Available online: https://nextcloud.lsasvcs.ipma.pt/s/SwRtreJqPPbrTc9 (accessed on 7 April 2023).
27. EUMETSAT Meteosat Satellites Are Spin-Stabilised with Instruments Designed to Provide Permanent Visible and infrared Imaging of the Earth. Available online: https://landsaf.ipma.pt/en/products/land-surface-temperature/lst/ (accessed on 7 April 2023).
28. EUMETSAT LSA SAF Algorithm Theoretical Basis Document for Land Surface Temperature (LST). Available online: https://nextcloud.lsasvcs.ipma.pt/s/MsmjYkwyQcApQMK (accessed on 7 April 2023).
29. Schwarz, N.; Lautenbach, S.; Seppelt, R. Exploring indicators for quantifying surface urban heat islands of European cities with MODIS land surface temperatures. *Remote Sens. Environ.* **2011**, *115*, 3175–3186. [CrossRef]
30. Wu, X.; Wang, G.; Yao, R.; Wang, L.; Yu, D.; Gui, X. Investigating Surface Urban Heat Islands in South America Based on MODIS Data from 2003–2016. *Remote Sens.* **2019**, *11*, 1212. [CrossRef]
31. Clinton, N.; Gong, P. MODIS detected surface urban heat islands and sinks: Global locations and controls. *Remote Sens. Environ.* **2013**, *134*, 294–304. [CrossRef]
32. Azevedo, J.A.; Chapman, L.; Muller, C.L. Quantifying the Daytime and Night-Time Urban Heat Island in Birmingham, UK: A Comparison of Satellite Derived Land Surface Temperature and High Resolution Air Temperature Observations. *Remote Sens.* **2016**, *8*, 153. [CrossRef]
33. Peng, J.; Xie, P.; Liu, Y.; Ma, J. Urban thermal environment dynamics and associated landscape pattern factors: A case study in the Beijing metropolitan region. *Remote Sens. Environ.* **2016**, *173*, 145–155. [CrossRef]
34. Chang, Y.; Xiao, J.; Li, X.; Frolking, S.; Zhou, D.; Schneider, A.; Wu, Y. Exploring diurnal cycles of surface urban heat island intensity in Boston with land surface temperature data derived from GOES-R geostationary satellites. *Sci. Total Environ.* **2021**, *763*, 144224. [CrossRef]
35. Meng, F.; Liu, M. Remote-sensing image-based analysis of the patterns of urban heat islands in rapidly urbanizing Jinan, China. *Int. J. Remote Sens.* **2013**, *34*, 8838–8853. [CrossRef]
36. Van Hove, L.W.A.; Jacobs, C.M.J.; Heusinkveld, B.G.; Elbers, J.A.; van Driel, B.L.; Holtslag, A.A.M. Temporal and spatial variability of urban heat island and thermal comfort within the Rotterdam agglomeration. *Build. Environ.* **2015**, *83*, 91–103. [CrossRef]
37. Fortuniak, K.; Kłysik, K.; Wibig, J. Urban–rural contrasts of meteorological parameters in Łódź. *Theor. Appl. Climatol.* **2006**, *84*, 91–101. [CrossRef]
38. Zhou, B.; Lauwaet, D.; Hooyberghs, H.; De Ridder, K.; Kropp, J.P.; Rybski, D. Assessing Seasonality in the Surface Urban Heat Island of London. *Am. Meteorol. Soc.* **2016**, *55*, 493–505. [CrossRef]
39. Yilmaz, S.; Menteş, Y.; Angin, S.N.; Qaid, A. Impact of the COVID-19 outbreak on urban air, Land surface temperature and air pollution in cold climate zones. *Environ. Res.* **2023**, *237*, 116887. [CrossRef]
40. AlDousari, A.E.; Kafy, A.A.; Saha, M.; Fattah, A.; Bakshi, A.; Rahaman, Z.A. Summertime Microscale Assessment and Prediction of Urban Thermal Comfort Zone Using Remote-Sensing Techniques for Kuwait. *Earth Syst. Environ.* **2023**, *7*, 435–456. [CrossRef]
41. Naikoo, M.W.; Islam, A.R.M.T.; Mallick, J.; Rahman, A. Land use/land cover change and its impact on surface urban heat island and urban thermal comfort in a metropolitan city. *Urban. Clim.* **2022**, *41*, 101052.
42. Koc, A.; Yilmaz, S. Landscape character analysis and assessment at the lower basin-scale. *Appl. Geogr.* **2020**, *125*, 102359. [CrossRef]
43. Gao, H.; Abu Bakar, S.; Maulan, S.; Mohd Yusof, M.J.; Mundher, R.; Zakariya, K. Identifying Visual Quality of Rural Road Landscape Character by Using Public Preference and Heatmap Analysis in Sabak Bernam, Malaysia. *Land* **2023**, *12*, 1440. [CrossRef]